Macromolecules

pubs.acs.org/Macromolecules Article

Mechanisms of Ion Transport in Lithium Salt-Doped Polymeric Ionic Liquid Electrolytes

Zidan Zhang, Amir T. Nasrabadi, Dipak Aryal, and Venkat Ganesan*

Cite This: *Macromolecules* 2020, 53, 6995−7008 Read Online

ACCESS | Metrics & More | Article Recommendations | Supporting Information

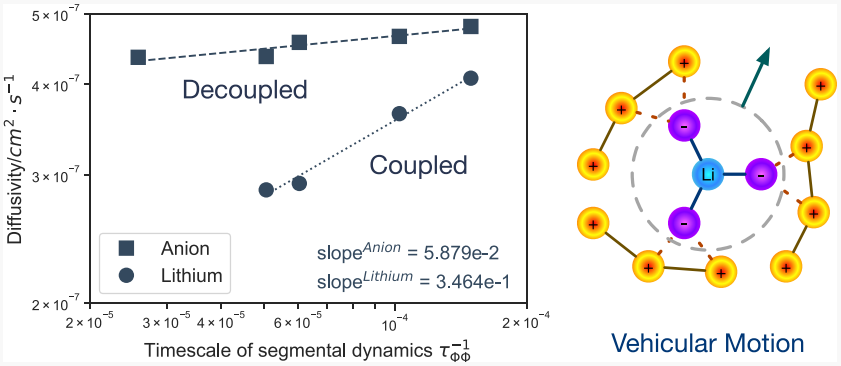

ABSTRACT: Recent experimental results have demonstrated that polymeric ionic liquids doped with Li salts exhibit enhanced ionic mobilities and lithium ion transference numbers with increasing salt concentrations. In this study, we used atomistic molecular dynamics simulations on a model system of lithium salt-doped 1-butyl-3-methyl-imidazolium bistriflimide ionic liquids and poly(1-butyl-3-methyl-imidazolium bistriflimide) electrolytes to identify the molecular mechanisms underlying such findings. Our results mirror qualitatively the experimental results on the influence of salt doping on the ion mobilities. Further, a surprisingly stronger dependence (coupling) between the lithium ion mobilities and polymer segmental dynamics is observed relative to the coupling between the anion diffusivities and polymer dynamics. We present results for ion coordination and hopping characteristics to rationalize such behaviors and identify the mechanistic origins of the properties of this emerging class of polymer electrolytes.

1. INTRODUCTION

Polymerized ionic liquids (polyILs) are macromolecules that incorporate traditional ionic liquid (monomeric IL) monomers as their repeating units. PolyILs inherit the unique physicochemical properties of ILs and the mechanical stability characteristics of solid polymer electrolytes, thereby endowing desirable performance features.[1−4] Among different applications, such materials are emerging of significant interest in pursuit of safe electrolyte materials for lithium ion batteries.[5−15]

Motivated by the desire to transition polyILs toward electrochemical applications, interest has arisen in the properties of lithium salt-doped polyILs.[16−22] In such a context, experiments have demonstrated that the dynamics of the free ion species (lithium ions and the counteranion of the polyIL) become faster with an increase in the concentration of lithium salt c_{Li}. Such trends are opposite the results noted in monomeric IL systems, in which the mobility of both lithium and anions decrease with an increase in the concentration of salt. Recently, Forsyth and co-workers reported the properties of poly(diallyldimethylammonium) bis(fluorosulfonyl)imide (PDADMA FSI) doped with bis(fluorosulfonyl)imide (LiFSI) salt[23] in which they again observed an increase in the diffusivities of both Li and the FSI ion up to a salt loading 1:2.0 mole ratio of PDADMA FSI:LiFSI. Interestingly, they observed that the salt concentration had a stronger influence on the lithium ion mobilities compared to that of the anions. As a result, the (ideal, diffusivity-based) lithium ion transference number, which measures the relative mobilities of the lithium and anions, increased and achieved an optimal at a 1:1.5 mole ratio.

Recent studies have identified a rich variety of mechanisms of ion transport in electrolyte systems. For instance, ion transport in salt-doped, neutral polymer electrolytes (such as PEO) has been extensively studied.[24−29] In such contexts, ion motion has been shown to involve polymer segmental motion-assisted hopping between the solvation sites of the electrolytes.[25,26,30] As a result, ion mobilities in such systems are strongly correlated to the polymer segmental dynamics and the glass transition temperatures.[25,26,30] Other recent works have also probed the

Received: June 19, 2020
Revised: July 27, 2020
Published: August 11, 2020

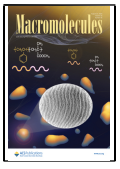

https://dx.doi.org/10.1021/acs.macromol.0c01444
Macromolecules 2020, 53, 6995−7008

mechanisms of ion transport in pure polyIL systems.[31−34] In such systems, the counterion motion was shown to also involve a hopping mechanism but involving delocalized interactions with the backbone grafted ions. As a result, the counterion motion in such systems were "partially" decoupled (i.e., exhibit a weaker correlation) from polymer segmental dynamics.[31]

Ion transport mechanisms in salt-doped monomeric ILs have also been studied extensively.[35−43] In such systems, the dynamics of all ion species (cation, anion, and lithium) become slower with increasing salt concentration. Such a behavior has attributed to the increased viscosity upon addition of salt, which results from the strong lithium−anion interactions.[36] Further, lithium ion transport in such systems has been shown to involve a combination of vehicular motion, in which lithium ion moves with its first solvation shell of anions, and structural diffusion, in which the anions on the first solvation shell refresh their identities frequently.[40,44,45] The former mechanism dominates when the lithium salt concentration (c_{Li}) is lower than 0.6, whereas the latter mechanism becomes more important when c_{Li} exceeds 0.6 (here the concentration c_{Li} is defined as the ratio of the number of lithium to the number of anions).[40,44,45]

Despite increasing interest in salt-doped polyILs, the mechanisms underlying ion transport in such systems remain poorly understood. In general, the salt-induced increases in ionic conductivity in such systems have been shown to be accompanied by a concomitant lowering of the glass transition temperature of the material, suggesting faster polymer dynamics to be a factor influencing the ion mobilities.[23,46] Forsyth and co-workers complemented their experimental results with molecular dynamics (MD) simulations, which indicated a co-coordination of the FSI anion with both the Li^+ ions and the polymer backbone, which they argued facilitates faster Li^+ transport.[23]

While the seminal study of Forsyth *et al.*[23] shed important insights on ion transport mechanisms in salt-doped polyILs, some unresolved issues remain. For instance, the manner by which co-coordination of anions facilitate faster ion transport is still not fully evident. Further, in many experimental studies, the anion mobilities exhibit a weaker dependence on salt concentration relative to the lithium ions.[23] The origins of such distinct behaviors of lithium and the anion mobilities also remain to be clarified. Finally, it is not evident if the ion transport mechanisms in salt-doped polyILs share features in common with the different electrolyte systems discussed above.

Motivated by the above issues, in the present study, we used atomistic molecular dynamics simulations to investigate and the ion transport mechanisms in a model salt-doped poly(1-butyl-3-methyl-imidazolium bistriflimide) electrolyte systems. Alongside, we also compare the structural details and transport mechanisms to those occurring in salt-doped 1-butyl-3-methyl-imidazolium bistriflimide (monomeric IL) electrolytes. Consistent with experimental results, we observed that, in polyILs, the addition of salt leads to an increase in the mobilities of both lithium and anions. Further, the anions exhibit a weaker dependence on salt concentration compared to the lithium ions, which leads to an increase in lithium ion transference numbers.[23] Our analysis demonstrates a stronger coupling between lithium ion motion and polymer segmental dynamics accompanied by a decoupling between the anion mobilities and polymer segmental dynamics. We characterize the structural details of our system which shed light on the ion transport mechanisms underlying the behavior of ion mobilities.

The rest of this article is organized as follows: in Section 2, we describe the setup of the polyIL and monomeric IL systems and the details of the quantification measures. In Section 3, we discuss the results of diffusion coefficients (Section 3.1), radial distribution functions (Section 3.2), influence of c_{Li} on the polymer segmental dynamics (Section 3.3), anion−cation/polycation associations (Section 3.4), and the lithium transport mechanisms (Section 3.5). We conclude with a brief summary of our findings and conclusions in Section 4.

2. SIMULATION DETAILS

All simulations in the current work were performed using the GROMACS 2018.4[47] MD software package. All the post-analyses were done by using the in-house code UTAnalysis, which is available upon request to the authors.

A series of salt-doped ionic liquid systems were prepared for the investigation of the influence of salt concentration on the ion transport mechanisms in the polyIL system and the monomeric IL system. The concentrations, c_{Li} (c_{Li} is expressed in terms of the ratio of the number of lithium ions to the number of cations/polycations), were chosen in the range of 0.0−0.4.

2.1. PolyIL System. We use the all-atom optimized potential for liquid simulations (OPLS-AA) for modeling the bond, angle, dihedral, and non-bonded interactions.[48] The initial configuration of a single polymer chain (poly(1-butyl-3-methyl-imidazolium bistriflimide)) template was prepared by using an adaptive resolution reverse mapping method.[49−55] In this procedure, we start with a coarse-grained representation of single polyIL chain (the mapping scheme accompanying the coarse-grained representation is shown in Figure 1) for

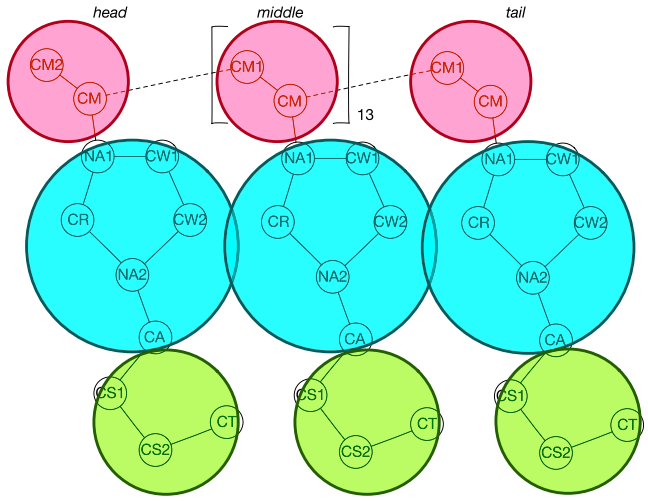

Figure 1. Each of the $BmIm^+$ monomer has been mapped into three coarse-grained beads, namely, the backbone bead (pink), the cation bead (cyan), and the tail bead (green); for simplicity, the hydrogens are not shown explicitly. The atom label at the atomistic resolution, the partial charges, and the force field parameters can be found in our previous work.[55]

equilibration. Subsequently, during the equilibration, the atomistic fragments are reintroduced by scaling the resolution of the atomistic level by a factor $\lambda(t)$:

$$\lambda(t) = \lambda_0 + \alpha(t - t_0),\ \{\lambda \in \mathbb{R};\ 0 \le \lambda \le 1;\ t_0 \le t \le t_{end}\} \quad (1)$$

https://dx.doi.org/10.1021/acs.macromol.0c01444
Macromolecules 2020, 53, 6995−7008

Here, λ_0 denotes the initial resolution, which is set to zero in our simulation, and α is the rate of change of the resolution, which was set to 0.001 in the current study. The resolution $\lambda(t)$ serves as a scaling factor that scales the potentials of the system:

$$U(\mathbf{r}, t) = \underbrace{\lambda^2(t)[U_{\mathrm{I}}^{\mathrm{AT}}(\mathbf{r}) + U_{\mathrm{II}}^{\mathrm{AT}}(\mathbf{r})] + U(\mathbf{r})_{\mathrm{III}}^{\mathrm{AT}}}_{\text{atomistic}} + \underbrace{[1 - \lambda^2(t)][U_{\mathrm{I}}^{\mathrm{CG}}(\mathbf{C}) + U_{\mathrm{II}}^{\mathrm{CG}}(\mathbf{C})]}_{\text{coarse-grained}} \quad (2)$$

Here U_{I} and U_{II} are the bonded and non-bonded potentials for the atomistic (AT) and coarse-grained (CG) scales, respectively. An additional interaction U_{III} is present only for the atomistic scale, which represents the bonded interactions that connects different CG beads. With the progress of the simulations, the resolution $\lambda(t)$ of the atomistic scale changes from 0 to 1, and due to the scaled potentials, the interactions between the coarse-grained beads and the atomistic fragments are coupled and adjusted. By using the above approach, the coarse-grained polymer chain is reverse mapped to its atomistic counterpart, after which a well sampled polymer chain is obtained. The force field parameters for both AT and CG scales and the spatial charges can be found in our recent work.[55]

For constructing the polyIL material, 20 atomistic polymer chains (15 monomers each) created from the above equilibration procedure are packed into a simulation box with corresponding number of TFSI anions and lithium ions (as listed in Table 1). The initial box length is 8 nm. A multi-step

Table 1. Simulation Details for Different Lithium Ion Concentrations c_{Li}[a]

species	BmIm	polyBmIm	TFSI	lithium
$c_{\mathrm{Li}} = 0.0$	300	20	300	0
$c_{\mathrm{Li}} = 0.1$	300	20	330	30
$c_{\mathrm{Li}} = 0.2$	300	20	360	60
$c_{\mathrm{Li}} = 0.3$	300	20	390	90
$c_{\mathrm{Li}} = 0.4$	300	20	420	120

[a]The total number of organic cations (BmIm monomer or the polyBmIm repeat unit) is fixed at 300.

equilibration procedure was used to prepare the equilibrated configuration for the production run:

1. 0.1 ns NVT simulation at 1000 K.
2. 0.1 ns NPT simulation at 600 K and 100 bar.
3. 0.1 ns NPT simulation at 600 K and 1 bar.

The above procedure was looped eight times to obtain the initial configuration for the production run. Such a pre-equilibrium procedure was inspired by the 21-step decompression method that has been proposed by Colina and co-workers.[56,57]

The production run of simulations were 110 ns long where the initial 10 ns was used for equilibration. The leap-frog algorithm was used as an integrator. The time step was set to 1 fs, the cutoff for the van der Waals was set to 1.3 nm, and the long-range electrostatic interactions were calculated with the particle mesh method.[58] In order to obtain better agreement of the dynamic properties between simulations and experiments, the partial charges of all atom species have been scaled by a factor of 0.8.[34,41,59−61] The temperature and pressure were set to 600 K and 1 bar, respectively. The V-rescale thermostat[62,63] and Parrinello−Rahman barostat[64] were used for temperature and pressure coupling, with the corresponding coupling parameters $\tau_T = 1.0$ ps and $\tau_P = 1.0$ ps. The default value of 4.5×10^{-5} bar was used as a compressibility constant for the barostat. All analysis that presented in the paper are averaged over 10 samples with different initial configurations.

2.2. Monomeric IL System. The structure and the force field parameters of ionic liquid 1-butyl-3-methyl-imidazolium bistriflimide ($[\mathrm{BmIm}]^+[\mathrm{TFSI}]^-$) were directly obtained from Acevedo and co-workers' works.[65,66] Different from their original version of parameters,[67] the partial charges in their second version of parameters was scaled by a factor of 0.8 to ensure consistency with our polyIL simulations.

2.3. Quantification Measures. *2.3.1. Diffusion Coefficient.* The transport properties of the ion species were probed by the diffusion coefficients that were derived from the corresponding mean square displacements (MSDs). The diffusion coefficient D_α (α = {anion, cation, or lithium ion}) can be calculated by using the Einstein relation

$$D_\alpha = \lim_{t \to +\infty} \frac{1}{6t} \langle (\vec{R}_\alpha(t) - \vec{R}_\alpha(0))^2 \rangle \quad (3)$$

where $\vec{R}$ is the position vector of the corresponding atom of species α.

For the anion (TFSI^-), the nitrogen atom is used as the reference to calculate the MSD, whereas, for cation 1-butyl-3-methyl-imidazolium (BmIm^+), the nitrogen atom that connects the butyl functional group was used to calculate the MSD. For the calculation of the MSD of lithium ion, we use the lithium atom itself. In our recent study, we found that, even with relatively long time simulation times extending 400 ns, polycation diffusivities are not easy to obtain for longer polymer chains.[68] Hence, in the present study, we neglect the diffusivity of polycations in the polyIL system.

Further, an "ideal" lithium ion transference number can be deduced based on the diffusivity:[24,69]

$$t_{\mathrm{Li}} = \frac{n_{\mathrm{Li}} D_{\mathrm{Li}}}{\sum_\alpha n_\alpha D_\alpha} \quad (4)$$

where $n_\alpha$is the number of ion species α. Again, the contribution arising from the mobility of polycations was ignored.

2.3.2. Radial Distribution Functions. The structural characteristics of the monomeric IL and polyIL systems were quantified by calculating the ion pair radial distribution function utilizing

$$g_{ij}(r) = \frac{V}{4\pi r^2 N_i N_j} \left\langle \sum_i^{N_i} \sum_j^{N_j} \delta(r - r_{ij}) \right\rangle \quad (5)$$

where N_i and N_j are the number of atoms of ion species i and j. V is the volume of simulation box, and δ is the Dirac delta function. The representative atoms chosen for anion, cation, and lithium were identical to those adopted for the analysis of diffusion coefficients. Further, the cutoffs for investigating the anion−cation/polycation and lithium−anion coordination were determined by the position r where $g(r) = 1.0$ after the first peak.

2.3.3. Polymer Chain Segmental Dynamics. To probe the segmental dynamics of the polyIL, we used the auto-correlation function of the dihedral angle of the backbone involving C−C−C−C atoms, which was calculated as[70−73]

$$C_{\Phi\Phi}(t) = \frac{\langle \cos \Phi(t) \cos \Phi(0) \rangle - \langle \cos \Phi(0) \rangle^2}{\langle \cos \Phi(0) \cos \Phi(0) \rangle - \langle \cos \Phi(0) \rangle^2} \quad (6)$$

https://dx.doi.org/10.1021/acs.macromol.0c01444
Macromolecules 2020, 53, 6995−7008

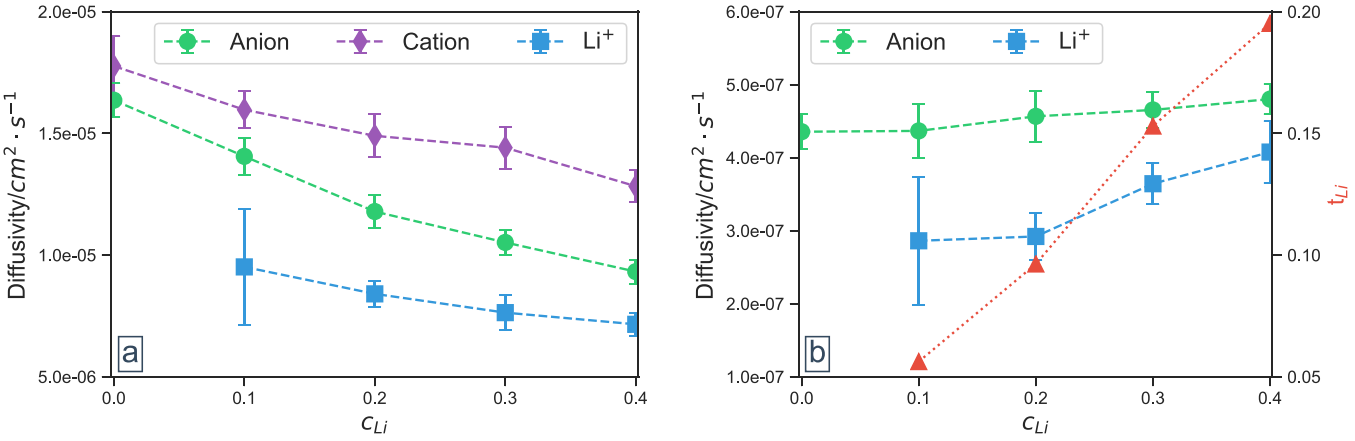

Figure 2. Diffusion coefficient for different ion species ((a) monomeric IL and (b) polyIL) as a function of lithium concentration c_{Li}. The ideal lithium ion transference numbers (eq 4) are indicated in (b).

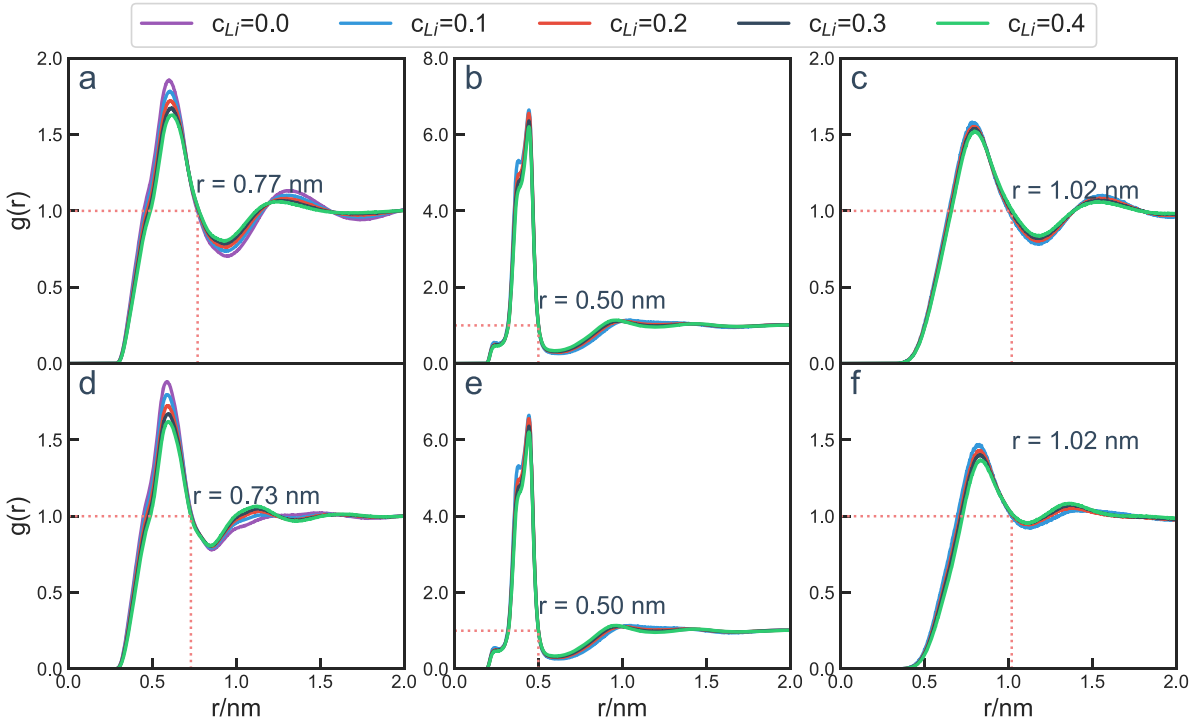

Figure 3. Radial distribution function for TFSI and $BmIm^+$ (left column), TFSI and Li (middle column), and $BmIm^+$ and Li (right column); the top panel is for the monomeric IL system, and the bottom panel is for the polyIL system.

where $\Phi(t)$ is the dihedral angle at time t and $\Phi(0)$ is the dihedral angle at the reference time. $C_{\Phi\Phi}(t)$ was fitted to a Kohlrausch–Williams–Watts (KWW) stretched exponential form[74−76]

$$C_{\Phi\Phi}(t) = \exp\left(-\left(\frac{t}{\alpha}\right)^{\beta}\right) \tag{7}$$

The relaxation timescale $\tau_{\Phi\Phi}$ of the segmental dynamics can be then calculated by using the following equation

$$\tau_{\Phi\Phi} = \alpha\Gamma\left(1 + \frac{1}{\beta}\right) \tag{8}$$

where Γ denotes the gamma function.

3. RESULTS AND DISCUSSION

3.1. Ion Diffusion Coefficients. We first discuss the results for the diffusion coefficient of the different ion species as a function of the concentration of the lithium salt. In Figure 2a, we display the results for monomeric ILs in which it can be seen that the mobility of all ion species decreases with increasing salt concentration. Such a trend has been reported in a number of prior experimental and simulation studies and has been attributed to the increased viscosity resulting from the addition of lithium salt.[36] The latter has been argued to arise from strong Li–anion interactions and the lithium clusters that form as a consequence in such systems.[40,77] In a prior study, we showed that similar features manifest in the context of protic ionic liquids.[78] To maintain brevity, in this article, we do not discuss further the mechanistic origins of the diffusivity results for monomeric ILs and instead focus only on the results for polyILs.

https://dx.doi.org/10.1021/acs.macromol.0c01444
Macromolecules 2020, 53, 6995−7008

In Figure 2b, we display the results for the diffusion coefficient of ions in the polyIL system (the corresponding "ideal" conductivities are presented in Figure S1 of the Supporting Information). In general, we observe that the ion diffusivities in polyILs are approximately 2 orders of magnitude smaller relative to monomeric ILs. Such results can be broadly understood to arise from the viscosity of the polyIL system and the slower dynamics of polymer chains. More pertinently, in contrast to the results for monomeric ILs, we observe that the diffusion coefficient of both the anions and the lithium increases with increasing salt concentrations. Further, we see that the anion diffusivities are much less sensitive to salt concentration compared to those of lithium ions. As a consequence, we observe that the "ideal" transference number t_{Li} (cf. eq 4) in polyIL increases with an increase in salt concentration (as shown in the secondary y axis in Figure 2b).

We note that the above results qualitatively accord with the trends reported in earlier experimental studies.[16,23,36] In such contexts, the increases in ion mobilities have been rationalized by demonstrating that the addition of salt lowers the T_g of the system.[16,23] Such effects have in turn been rationalized by arguing that the presence of lithium ions reduces the coordination between the anions and polycations and instead increases the coordination of anions with the lithium ions. Simulation results presented by Forsyth and co-workers for PDADMA FSI doped with LiFSI salt supported such a hypothesis by showing that the co-coordination between anions and lithium increases with an increase in salt concentration.[23]

The remaining parts of this results section seeks to unravel the origins of our simulation results by considering a multitude of equilibrium and dynamical features. Toward this objective, we divide our ensuing discussion into three major parts:

1. The influence of salt concentration on polymer segmental dynamics and the role of anion coordination characteristics upon such features.
2. The mechanistic origins of the dependence of anion diffusivities on salt concentrations.
3. The mechanistic origins of the dependence of lithium diffusivities on salt concentrations.

3.2. Radial Distribution Functions. The results presented in the subsequent sections rely substantially on the coordination characteristics of the different ions deduced using the radial distribution functions (RDFs). Preliminary to such a discussion, we present the results for the RDFs of both monomeric IL and polyIL in Figure 3. From the results, we see that, in both monomeric IL and polyIL, increasing salt concentrations lead to a reduction of the peak intensity, which is consistent with the expected screening of the electrostatic interactions. Further, it is observed from Figure 3a,d that the height of the first peak for TFSI and $BmIm^+$ are almost identical for monomeric IL (a) and polyIL (d). However, the second peak in polyIL is seen to emerge at a closer distance in comparison to monomeric IL. Correspondingly, in comparing the interactions between cation/polycation with Li, the second peak in Figure 3f is seen to be shifted to the left when compared to Figure 3c. Similar results were observed in our recent study on IL-polyIL blends[79] and can be rationalized as a consequence of the polymer backbone connectivity inducing stronger anion−polycation interactions in polyIL systems.

Important information that can be obtained from $g(r)$ is the distance of the first coordination shell, which can be used to analyze the coordination of ion pairs. Explicitly, we chose the position where $g(r)$ equals 1.0 after the first peak as a measure of the distance at which two ions are considered to be coordinated. From Figure 3, we see that the cutoffs for TFSI and $BmIm^+$/$polyBmIm^+$ are 0.77 and 0.73 nm, respectively. Again, the shorter cutoff in polyIL in comparison to monomeric IL can be attributed to the closer distance between polycations in the former system. However, the cutoffs for ion pairs TFSI-Li (0.5 nm) and $BmIm^+$/$polyBmIm^+$-Li (1.02 nm) are almost identical when comparing monomeric IL to polyIL.

3.3. Influence of Salt on Polymer Segmental Dynamics. As discussed in Section 1, previous studies have attributed the salt-induced increase in ion diffusivities of polyILs to an acceleration of polymer segmental dynamics and the reduction in T_g of such systems.[16,23] To probe if similar effects manifest in our system, we examined the timescale of backbone dihedral auto-correlation function $\tau_{\Phi\Phi}$ of the polymer as a measure of the polymer segmental dynamics (cf. eq 8; the fitting of the backbone dihedral auto-correlation function $C_{\Phi\Phi}(t)$ is presented in Figure S2, Supporting Information).

As seen in the results displayed in Figure 4, $\tau_{\Phi\Phi}$ decreases monotonically with increase in c_{Li}, indicating that the addition of salt indeed facilitates faster segmental dynamics of the polymer chains. As discussed earlier, prior studies have rationalized such observations by suggesting that the addition of salt reduces the extent of coordination between the anions and the cations while increasing the coordination of the anions with the lithium ions. To analyze such effects in our system, we turn to the anion coordination characteristics.

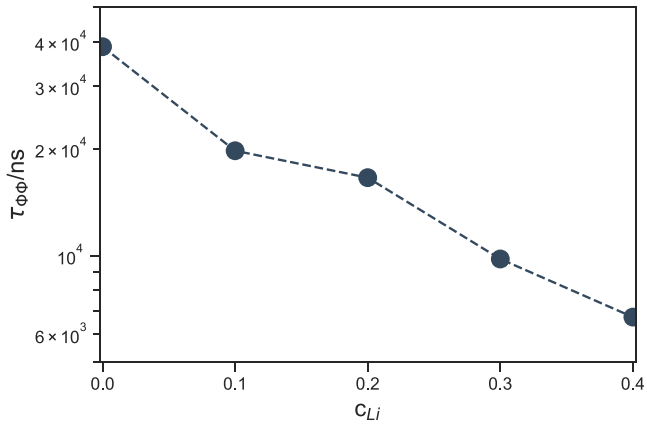

Figure 4. Dependence of backbone relaxation time $\tau_{\Phi\Phi}$ on the lithium concentration c_{Li}.

We categorize the anion coordination in polyILs into three groups: (i) anions that are only associated with the (poly)cation (henceforth in this article, we term this category as Type1 anions), (ii) anions that are associated with both cation and Li (such anions will be referred to as Type2 anions), and (iii) anions only associated with Li ions (referred to as Type3 anions) (cf. Figure 5).

The results for the ion coordination statistics for both monomeric IL and polyIL are displayed in Figure 6a. In both systems, it is observed that the fraction of anions only associated with cation (Type1) decreases with an increase in c_{Li}. In contrast, the fraction of anions associated simultaneously with both cation and lithium (Type2) increases with c_{Li}. Interestingly, for the concentrations examined in this work, the number of ions that are only associated with Li (Type3) is seen to be very small.

https://dx.doi.org/10.1021/acs.macromol.0c01444
Macromolecules 2020, 53, 6995−7008

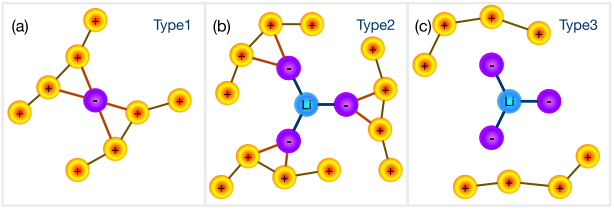

Figure 5. (a) Type1 anions, which are only associated with the (poly)cation; (b) Type2 anions, which are associated with both cation and Li; and (c) Type3 anions, which are only associated with Li ions.

The above results are intuitive and can be understood based on the increased presence of the oppositely charged lithium coordination centers for the anions. Further, as discussed in Section 2.3 (cf. Figure 3), the interactions between anions and lithium are seen to be stronger than those between anion and cations, which explains the preference for the anions to associate with the added lithium. Slight differences can be noted between monomeric IL and polyIL systems, in that the Type1 coordination of monomeric IL is seen to be lower than that in polyIL, and correspondingly, the Type2 coordination of monomeric IL is slightly higher than that in polyIL. Such differences can be rationalized by the fact that the connectivity of the polymer backbone in polyILs places more cations in proximity to each other, thereby increasing the likelihood of anion coordinations with the cation.

While the above result is consistent with the hypothesis proposed for the influence of salt on polymer dynamics,[23] a more direct explanation is provided by the disruption of cation−anion−cation "bridges" arising from the addition of salt. An illustration of an intermolecular cation−anion−cation bridge is displayed in Figure 6b, where we can see that a given anion is associated with five polycations from three polymer chains and seven bridges (three bridges each between chains 1 and 2 and one bridge between chains 2 and 3) are formed. Such bridges can be viewed as physical "cross-links" between the different polymer chains, and their disruption can be used to rationalize the faster polymer segmental dynamics.

In Figure 6c, we display the number of intermolecular cation−cation coordinations arising from the Type1 and Type2 anions. As can be seen from the results, the number of bridges arising from Type1 coordinated anions decreases and that arising from Type2 coordinated anions increases with increasing salt concentration. More pertinently, the total number of cation−cation bridges is seen to decrease with an increase in salt concentration.

Together, the above results provide a microscopic explanation for the influence of salt on the polymer dynamics. As suggested in prior studies, the addition of salt is indeed seen to increase the

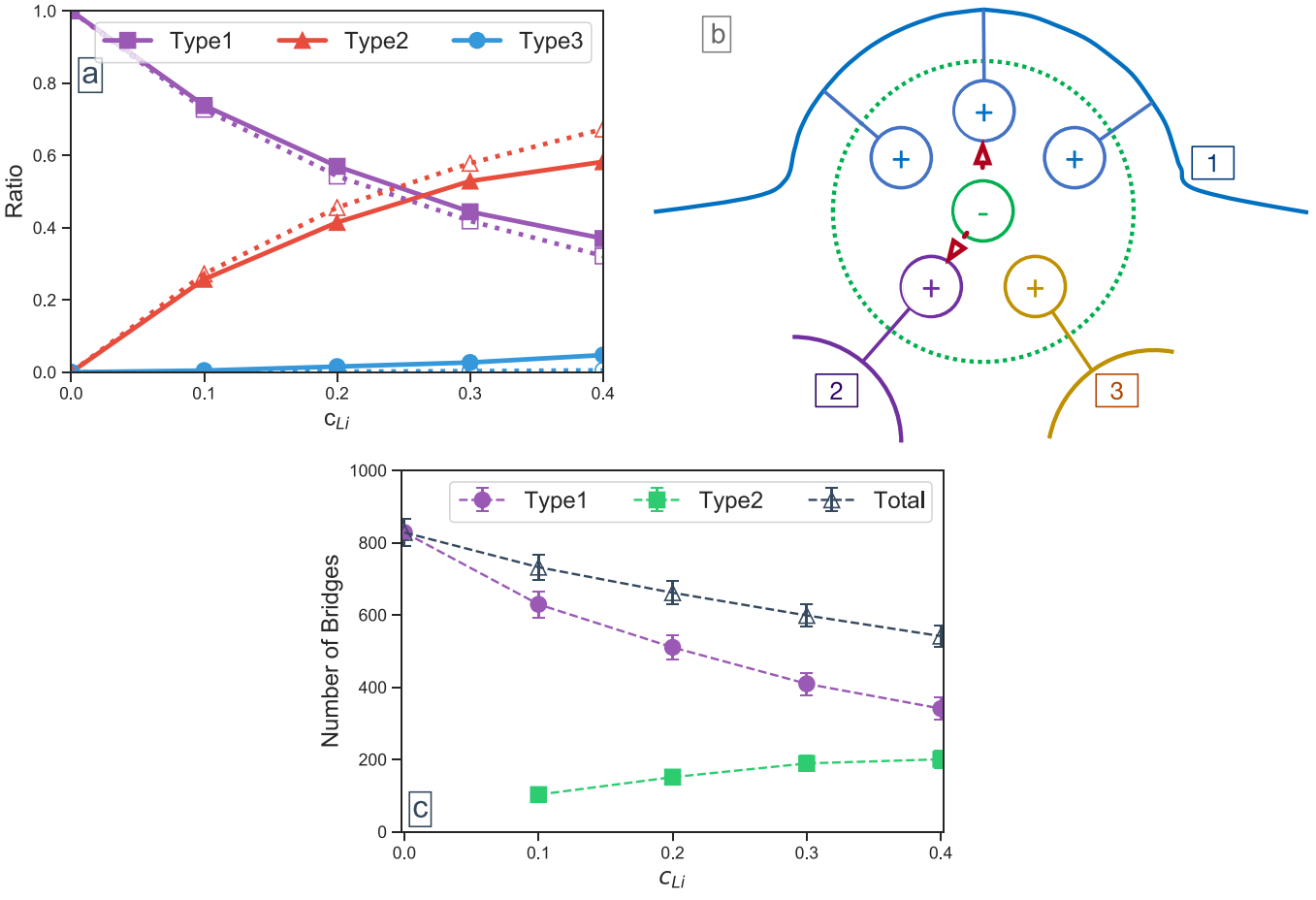

Figure 6. (a) Fraction of different TFSI coordination types (normalized by the total number of TFSI associations) for polyIL (solid) and monomeric IL (dotted). (b) Illustration of a polycation−anion−polycation bridge; a given anion is associated with three polymer chains, and the bridge is formed between cations from chain 1 to 3. We count only bridges arising between intermolecular cations. (c) Number of polycation−anion−polycation bridges connecting different polymer chains through Type1 and Type2 associations.

https://dx.doi.org/10.1021/acs.macromol.0c01444
Macromolecules 2020, 53, 6995−7008

extent of co-coordination between anion and lithium at the expense of the coordination between anions and cations. Such changes in anion coordination are seen to decrease the total number of cation−anion−cation bridges. Together, such coordination features serve to rationalize the faster polymer segmental dynamics arising from the introduction of salt.

Having discussed the origin of faster polymer dynamics, we turn now to the dependence of the ion mobilities on polymer segmental dynamics. In Figure 7, we display the ion (anion and

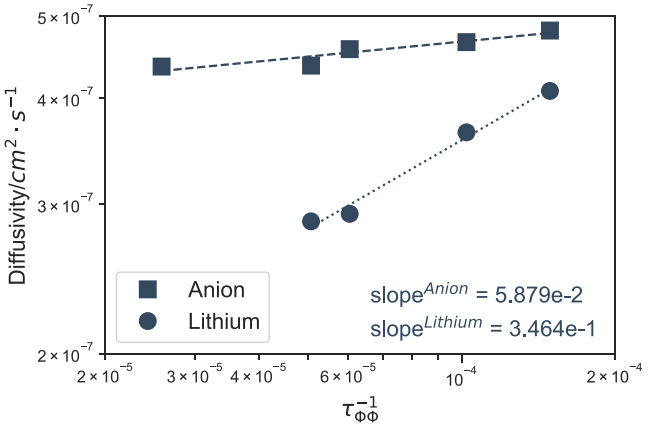

Figure 7. Dependence of diffusion coefficient of anion and lithium on $\tau_{\Phi\Phi}^{-1}$. The annotations list the exponents of the power law fit to the diffusivities.

Li) mobilities as a function of the backbone relaxation time $\tau_{\Phi\Phi}$. Therein, we observe a surprising result, viz., that the anions, which are directly coordinated to the polymer chains, exhibit only a weak dependence ("decoupled") between the mobilities and $\tau_{\Phi\Phi}$. In contrast, lithium ions, which are only indirectly coordinated with the polymer chains, are seen to exhibit a stronger dependence ("coupled") on $\tau_{\Phi\Phi}$. We note that such results directly relate to the salt concentration dependencies of the mobilities of anions and cations seen in Figure 2 and the accompanying increase in the lithium ion transference numbers. In the next two sections, we consider the coordination characteristics and the mechanistic origins of these unusual decoupling/coupling behaviors of the mobilities of the anions and lithiums.

3.4. Anion Transport Mechanisms. To understand the origin of decoupling between anion mobilities and polymer dynamics, we undertook a detailed consideration of the coordination statistics and hopping events of the anions. To understand the influence of salt on the TFSI coordination characteristics, we calculated the probability, $P(n)$, that a given TFSI is associated with n cations/polycations. The corresponding results are displayed in Figure 8 at different c_{Li} at 600 K. In the polyIL system, it is observed from Figure 8a that $P(n)$ exhibits a maximum at $n = 4$ in the absence of Li salt.[31] However, as the c_{Li} increases, the location of the peak is seen to gradually shift to $n = 3$, while the association with four cations constitutes the second major coordination group.

We hypothesize that the above results reflect a combination of the coordination characteristics of the Type1 and Type2 anions. To verify this proposal, we divided the $P(n)$ coordination statistics of TFSIs into those specific to the Type1 and Type2 subgroups (Figure 8b,c). It is seen in Figure 8b that increasing c_{Li} has a negligible influence on $P(n)$ of Type1 anions. In contrast, as seen in Figure 8c, the coordination behavior of Type2 anions display peaks of $P(n)$ at $n = 3$ and $n = 2$, suggesting that such anions swap out either one or two cations and engage with lithium as a third and/or fourth partner for their coordination. Together, the results of Figure 8b and Figure 8c confirm that the coordination characteristics presented in Figure 8a arise from a combination of the association behaviors of Type1 and Type2 anions. More pertinently, we observe that the coordination behaviors of Type1 anions are not influenced by the salt concentration.

In Figure 8e,f, as a comparison, we display the corresponding results for the influence of salt on the coordination characteristics of monomeric ILs. In comparing with the results of Figure 8a−c, we observe very similar features to those observed for polyILs. Explicitly, based on $P(n)$ shown in Figure 8d, we observe that a maximum of $P(n)$ at $n = 4$ is observed at low salt concentrations, which then shifts toward $n = 3$ at higher salt concentrations. The examination of the coordination characteristics of the two TFSI subgroups displayed in Figure 8e and Figure 8f again confirms that the results of Figure 8d can be attributed to the influence of the Type2 anions and that Type1 anions preserve their coordination features even in the presence of salt.

Next, we turn to the influence of salt on the coordination of anion with distinct polymer chains. We quantify such features through the consideration of the probability $P(N)$ that an anion is coordinated with N distinct polymer chains. The results of $P(N)$ for the anion and its two subgroups are presented in Figure 8g−i. Consistent with our other studies,[31] a peak of $P(N)$ at $N = 2$ is observed in the absence of Li salt. Further, with an increase in c_{Li}, the peak is seen to transition from $N = 2$ to $N = 1$. Again, such results can be understood based on the coordination behaviors of Type1 and Type2 anions. From the results displayed in Figure 8i, the Type2 anion is seen to preferentially associate with a single polymer chain. In contrast, for Type1 anions in Figure 8h, we observe that the presence of lithium salt has only a slight influence on $P(N)$ of such ions.

Together, the results discussed above indicate that the coordination characteristics of anions in polyILs arise from a combination of the features exhibited by Type1 and Type2 ions. Among these, Type1 ions are seen to retain the characteristics exhibited by anions in pure polyILs (i.e., in the absence of salt).[31] In contrast, Type2 anions exhibit a coordination with one polymer chain and fewer cations. Together, the results of the coordination statistics presented in Figure 8 suggest that the co-coordinated anions dissociate from the second polymer chain and instead preferentially engage in coordination with the cations of a single polymer chain. Moreover, such Type2 anions only associate two or three cations and swap some of their original (Type1) associations to Li ions.

As a last piece of information to understand the dynamics of Type1 and Type2 anions, we probed the possible modes/events by which the anions move along the polymer chain(s). We note that a Type1 anion can move by one of two possible hopping processes: (i) by breaking a bond (i.e., coordination) with a cation and forming a new bond with another cation (in such a case, the identity of the anion remains as Type1) or (ii) the anion can break a coordination with a cation and instead coordinates with a lithium ion and become a Type2 anion. Similarly, a Type2 anion can also move by one of two possible hopping processes: (i) the anion breaks the bond with the cation and forms a new bond with another cation and remains as Type2 or (ii) the anion breaks a coordination with a lithium and instead coordinates with a cation to become a Type1 anion.

https://dx.doi.org/10.1021/acs.macromol.0c01444
Macromolecules 2020, 53, 6995−7008

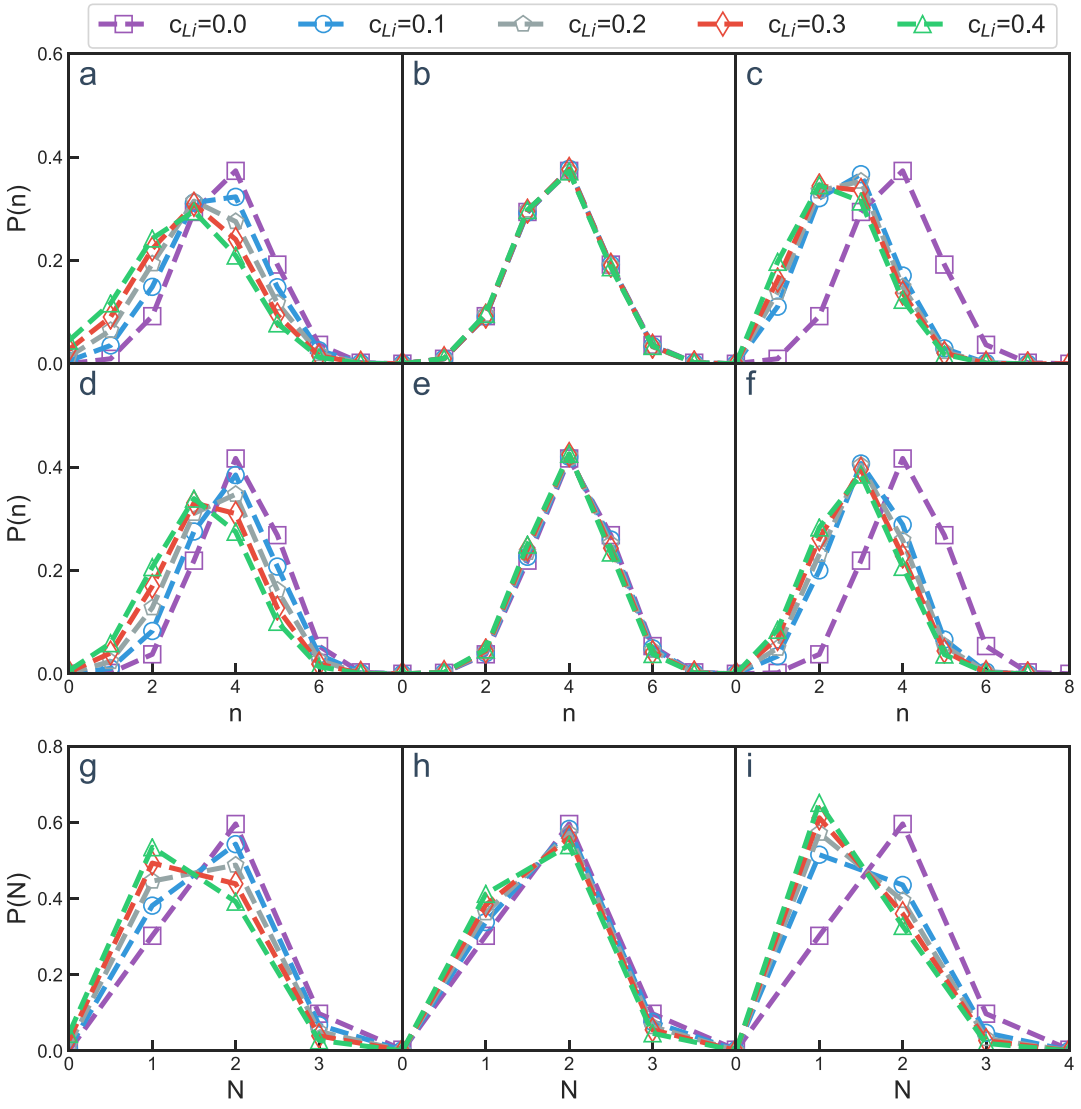

Figure 8. (a–f) Probability that a given TFSI is associated with *n* cations: (a–c) polyILs and (d–f) monomeric ILs. (g–i) Probability that a given TFSI is associated with the *N* polymer chains.

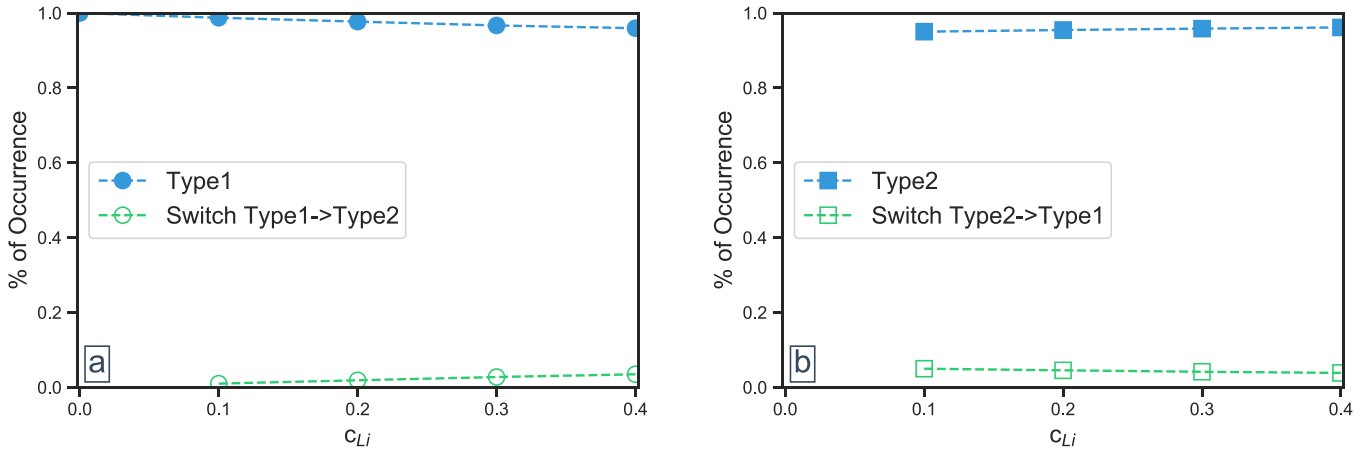

Figure 9. Probability of hopping events for (a) Type1 and (b) Type2 anions. The solid (open) symbols pertain to the probability that a given anion retains (changes) its identify after hopping.

In Figure 9a, based on frame analysis of our simulations (the details of the methodology are discussed in the context of Figure S3 of the Supporting Information), we display the respective fractions of Type1 anions, which hops but remains as Type1, and those that hop and become a Type2 anion (these fractions have been normalized by excluding the inactive fraction of anions, i.e.,

https://dx.doi.org/10.1021/acs.macromol.0c01444
Macromolecules 2020, 53, 6995–7008

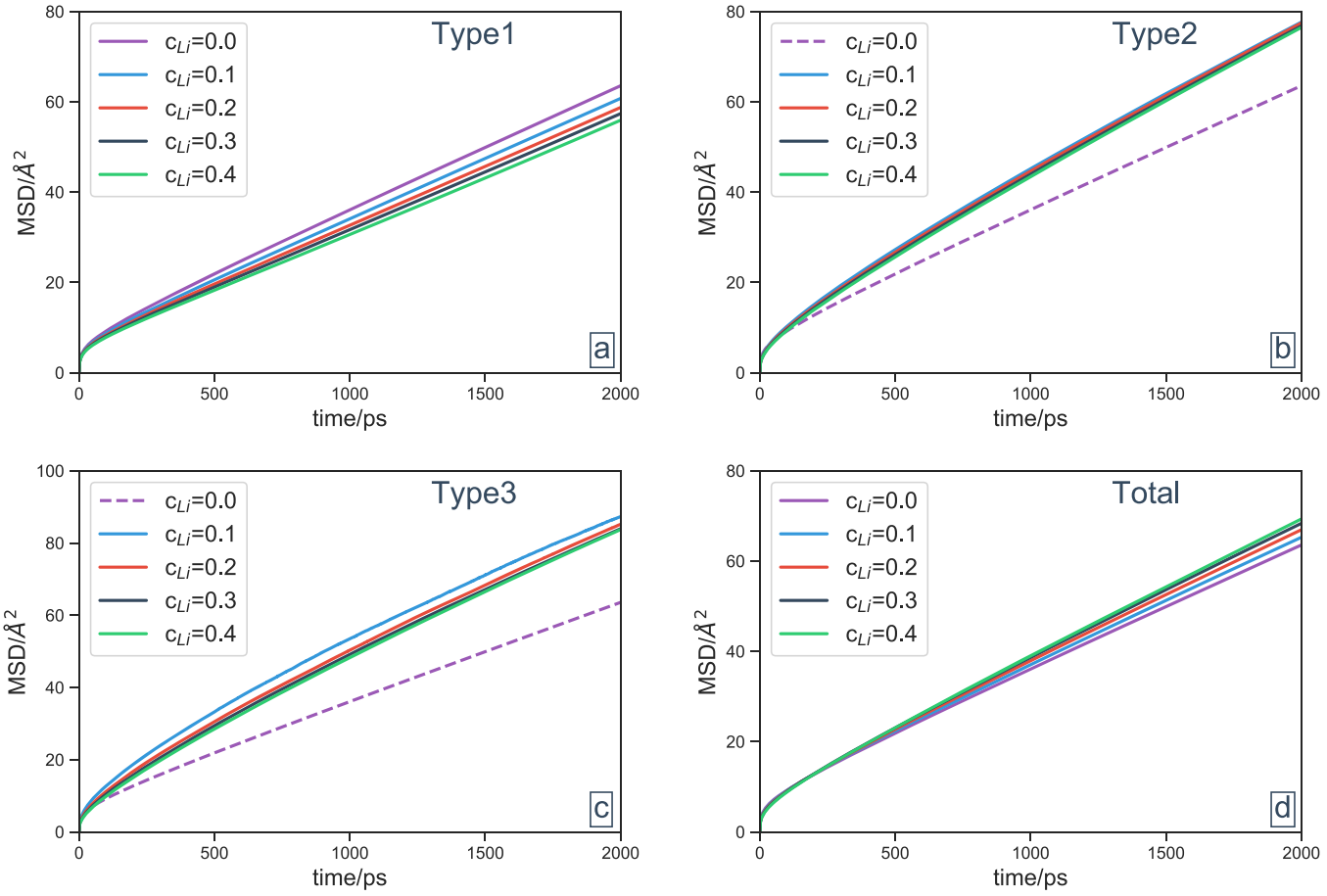

Figure 10. Short-time mean square displacements for (a) Type1 anions, (b) Type2 anions, (c) Type3 anions, and (d) all anions. For (b) and (c), there is no corresponding type of anions in c_{Li} = 0.0, and hence the results for c_{Li} = 0.0 is borrowed from (a) and displayed as a benchmark.

those that do not hop during the time frame of analysis). For the salt concentrations probed in the study, we observe that the majority of Type1 anions move by a mechanism that retains their identity. The fraction of anions that switch from Type1 to Type2 is seen to increase with increasing salt concentration, but the fraction still remains to be less than 0.05 for the highest salt concentrations probed. In Figure 9b, we display the corresponding results for Type2 anions wherein we observe similar trends, suggesting that the majority of the ions retain their identities during their motion.

Based on the above results, we propose a tentative explanation for the influence of salt on the dynamics of anions as arising from the differing influences of salt on the dynamics of Type1 and Type2 anions. Specifically, since the Type1 anions exhibit coordination characteristics identical to those in pure polyILs and also retain their identity during hops, the transport mechanism of such ions is expected to be identical to that identified for pure polyILs.[31] Specifically, in our earlier studies, the ion hopping pathways for anions in pure polyILs were found to involve correlated hopping of the different ions[31,68] accompanied by the breaking and formation of new intra- and intermolecular associations, which preserves the coordination characteristics of the ions. However, as our results in Figure 8 demonstrate, in the presence of Li salt, such pathways are expected to be hindered due to the existence of Type2 anions exhibiting distinct coordination characteristics. As a result, we expect the dynamics of the Type1 anions to become slower with increased salt concentrations. In contrast, since the Type2 ions require only one polymer chain for its coordination and hopping, their pathways are much less impacted by the presence of Type1 ions. Further, since such anions are (mostly) coupled to a single polymer chain, their dynamics is expected to be faster than Type1 anions.

To support our above hypothesis, we probed the short-time mean square displacements (MSDs) of Type1 and Type2 anions (in Supporting Information, Figure S4, we present the results for the association timescale between the Type1, Type2 anions and the cations to demonstrate that the majority of the anions retain their original identity in the timescale probed for the short-time MSDs). In the results displayed in Figure 10, we observe that the Type1 anions become slower as the lithium concentration (c_{Li}) increases. For Type2 anions, while no perceptible trend is evident regarding the influence of salt concentrations, it is clear that such anions are significantly faster than Type1 anions. Similarly, Type3 anions (albeit constituting only a small fraction of the overall population) are also seen to be significantly faster than the Type1 ions. As a further evidence, the cation−anion association timescales displayed in Supporting Information, Figure S4 also demonstrate a much slower relaxation (i.e., longer-lived associations) for Type1 anions compared to Type2 anions.

Together, the above results demonstrate that the weak salt concentration dependence of the mobility of the anions can be understood to arise as a result of a "compensation" effect between the slower dynamics of Type1 ions and the faster dynamics (and increasing populations) of Type2 ions. The net

https://dx.doi.org/10.1021/acs.macromol.0c01444
Macromolecules 2020, 53, 6995−7008

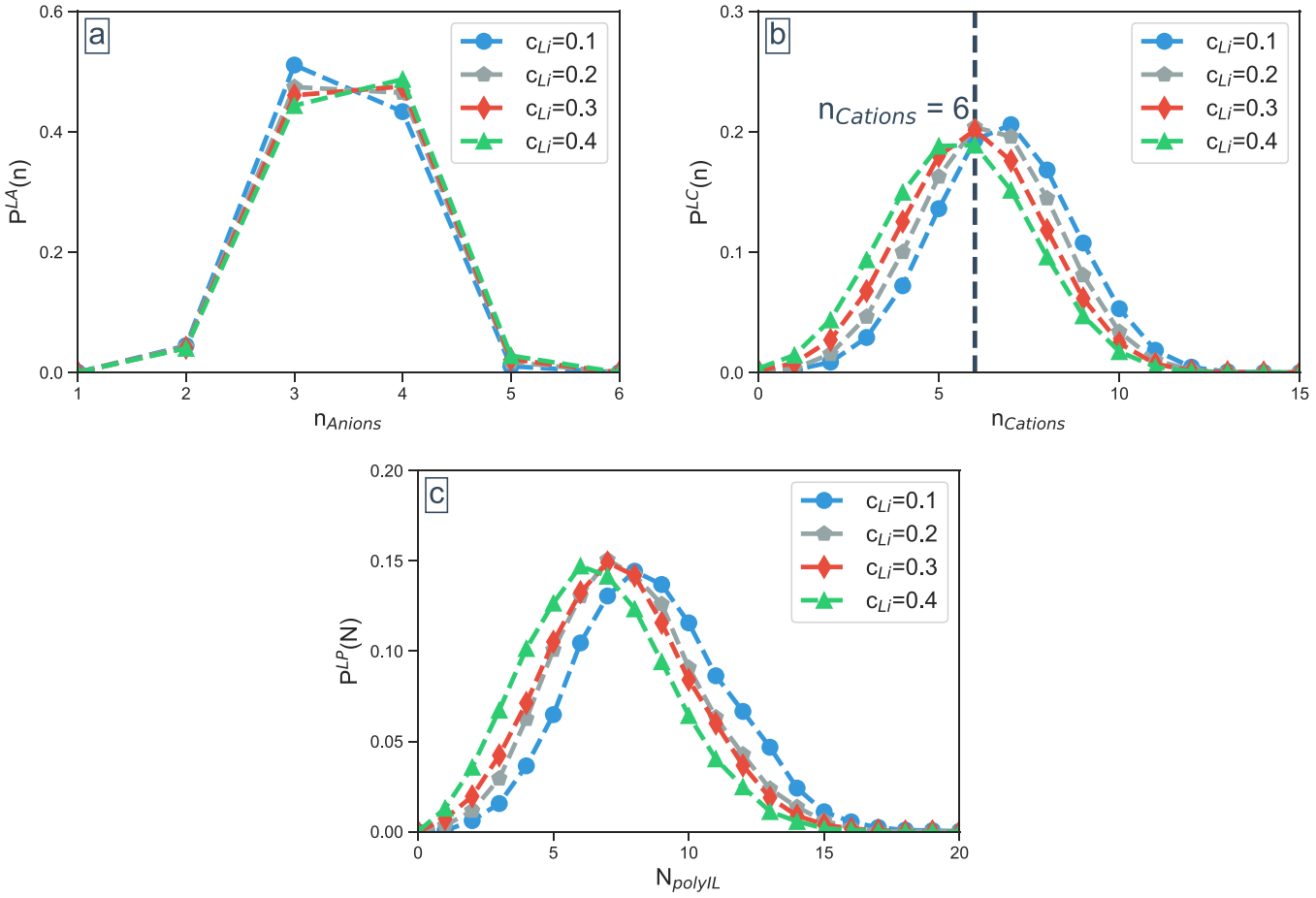

Figure 11. (a) Probability $P^{LA}(n)$ that a given Li is associated with n TFSI for polyILs. (b) Probability $P^{LC}(n)$ that a given Li is associated with the number of cation for polyILs through the Li−anion−cation co-coordination. (c) Probability $P^{LP}(n)$ that a given Li is associated with the number of polymer chains.

anion dynamics, which reflects the combination of faster Type2 and slower Type1 ions, appears only weakly coupled to the polymer segmental dynamics.

3.5. Lithium Ion Transport Mechanisms. In this section, we present results for the coordination characteristics and the mechanisms of lithium ion motion to clarify the origins of the coupling between the mobilities of the lithium ions and the polymer segmental dynamics. To place our discussion below in context, we note that a number of earlier studies[35,36,38,40] have probed the mechanisms of lithium transport in salt-doped pure monomeric ILs and have deduced two broad categories of motion: (a) vehicular motion, in which lithium ion moves with its first solvation shell of anions, and (b) structural diffusion, in which the anions on the first solvation shell of lithium refresh their identities frequently and lithium ions move akin to a hopping mechanism between the anions. It has been suggested that, in polyILs, the co-coordination of Li with anions facilitates an anion hopping mechanism of Li.[23] Further, such hopping transport has been hypothesized to be the origin of salt-induced increased Li mobilities in polyILs.

To characterize the Li−anion coordination behavior in polyIL systems (the corresponding results for monomeric IL systems are presented in Figure S5 of the Supporting Information), in Figure 11a, we present results for $P^{LA}(n)$, the probability that a given Li ion is coordinated with n anions. The peak of $P^{LA}(n)$ at the lowest salt concentration is seen at $n = 3$, which indicates that a given Li preferentially associates with three anions. With increasing salt concentration, the probability distributions are seen to exhibit comparable magnitudes of peaks at $n = 3$ and $n = 4$. In Figure 11b, we display results for the probability $P^{LC}(n)$ that a given Li ion is associated with n cations indirectly through the anions. For low salt concentrations, the peak of the probability distribution is seen to occur at six cations. With an increase in salt concentration, the peak of the probability distribution is seen to move toward fewer cations, reflecting closely the coordination characteristics of Type2 anions (cf. Figure 8c). Finally, in Figure 11c, we present results for the probability distribution of the number of distinct polymer chains to which a Li ion is indirectly associated. Therein, it is seen that each lithium ion is indirectly coupled to an order of 5 − 10 distinct polymer chains.

Together, the results of Figure 11 suggest a picture in which the Li ions in polyILs (and monomeric ILs, which exhibit similar coordination characteristics as discussed in Supporting Information, Section S5) and a given Li ion are resident in a big cluster, where it is surrounded by multiple anions in the first solvation shell and by multiple polycations on the outer sphere of the first solvation shell.

To quantify the mechanisms of motion of lithium ions, we decomposed the transport events of Li into two main categories as schematically illustrated in Figure 12: (i) Vehicular (Figure 12a,b): In this case, the anion which is associated with the lithium breaks a coordination with its associated cation (or multiple associations with different cations) and forms new

https://dx.doi.org/10.1021/acs.macromol.0c01444
Macromolecules 2020, 53, 6995−7008

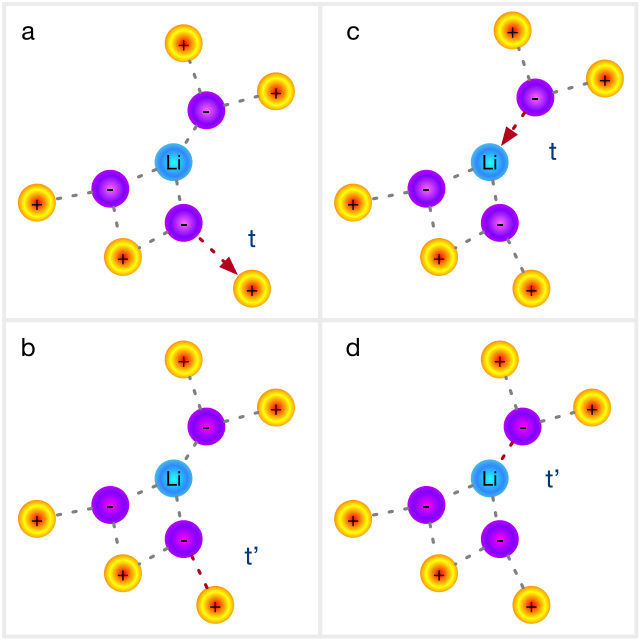

Figure 12. Two types of hopping events that are involved in the newly formed co-coordination. The red arrow indicates the potential association at time t, and the red dashed line indicates that the potential association at time t has converted to a newly formed association at time t'. (a, b) The vehicular hopping event that the new association is formed between cation/polycation and anion. (c, d) The structural hopping event that the new association is formed between lithium and anion.

associations with different cation(s). In this mode of transport, lithium moves with the anions in its solvation shell. (ii) Structural (Figure 12c,d): This relates to motions in which the lithium breaks its coordination with the anion and forms a new coordination with a different anion. This motion is akin to a hopping motion of lithium facilitated by the anions.

The results for vehicular and structural events for polyIL and monomeric IL systems are displayed in Figure 13. For the monomeric IL system, it is observed that the vehicular events constitute the dominant mechanism of transport for the salt concentrations considered in this study. More explicitly, the

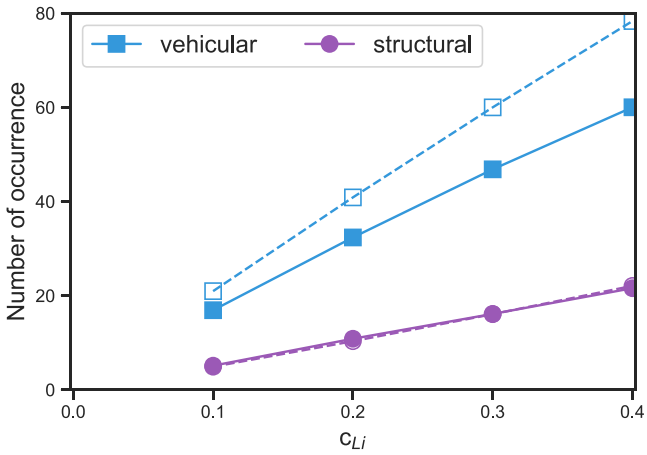

Figure 13. Number of occurrence of vehicular (square) and structural (circle) hopping events as a function of lithium concentration c_{Li} for polyIL (solid line) and monomeric IL (dashed line).

number of vehicular events is seen to be approximately four times that of the structural hopping events. Such results are in accord with earlier reports, which have noted vehicular diffusion to be the dominant mechanism of lithium ion transport at low salt concentrations.[40] More surprisingly, the results of the hopping events in the polyIL system (Figure 13) are seen to be similar to that in the monomeric IL system and that the vehicular events still constitute the dominant contribution to the overall hopping events. However, the actual number of vehicular events in polyILs is seen to be lower than monomeric ILs, reflecting the overall slower transport of Li ions. In both monomeric IL and polyIL systems, it is observed that all types of hopping events increase with salt concentration due to the decreased ion pair interactions.

The results of Figure 13 suggests a framework in which, in both monomeric IL and polyIL systems, the Li ions primarily move along with the anions in the first solvation shell while refreshing the cations/polycations to which the anions are connected (vehicular motion). In such a framework, to explain the dependence of the mobility of Li ions on salt concentration and polymer segmental dynamics, we invoke the results of Figure 11c, which suggests that, while the Li ions themselves are not directly connected to the polymer chains, through the Li−anion−polycation bridges, the Li ion is "connected" to multiple polymer chains. As a result, the motion of the Li ion (along with its solvating anions) is expected to be influenced by the dynamics of the surrounding medium and the polymer chains. We propose that this picture constitutes the mechanism underlying the coupling between the lithium ion mobilities and the timescale of polymer segmental dynamics (Figure 7).

4. SUMMARY AND CONCLUSIONS

In summary, in this article, we presented results of atomistic molecular dynamics simulations studying ion mobilities and the molecular mechanisms of transport in lithium salt-doped 1-butyl-3-methyl-imidazolium bistriflimide ionic liquids and poly(1-butyl-3-methyl-imidazolium bistriflimide) electrolytes. Our results mirrored the qualitative features of experimental results on the influence of salt doping on anion and lithium diffusivities.

The addition of salt to polyILs was seen to increase the extent of co-coordination between anion and lithium at the expense of the coordination between anions and cations. Such changes in anion coordination was seen to decrease the total number of cation−anion−cation bridges and led to faster polymer segmental dynamics. However, our results indicated a surprisingly stronger dependence (coupling) between the lithium ion mobilities and polymer segmental dynamics relative to the dependence of anion diffusivities on polymer dynamics. Based on coordination and hopping analysis, we deduced that the anion dynamics reflected an average of the slower dynamics of ions, which were coordinated only to the cations and the faster dynamics of ions co-coordinated with both cations and lithium. The Li ions were shown to move primarily by vehicular motion along with its solvating anions for the salt concentrations probed in our study. The coupling between the Li ion motion and polymer segmental dynamics was rationalized by demonstrating that the Li ions were indirectly coordinated to a number of polymer chains through its solvating anions. As a result, the dynamics of the surrounding medium (i.e., the polymer chains) was argued to couple to the motion of the Li ion.

The present study serves to identify the mechanistic aspects of coordination and transport in salt-doped polyILs, a class of

https://dx.doi.org/10.1021/acs.macromol.0c01444
Macromolecules 2020, 53, 6995−7008

electrolytes which are emerging to be of significant interest for lithium ion battery applications. Our results suggest that the features underlying such systems share commonalities with both pure polyILs (i.e., in the absence of salt) and other salt-doped electrolyte systems. Indeed, the coordination and transport behavior of Type1 ions identified in our simulations was seen to mirror the behaviors noted for pure polyILs.[31−34] In contrast, the coordination and transport behavior of Type2 ions and the lithium ions that were coordinated to such anions resembled the characteristics of other salt-doped polymer electrolytes in their coupling to polymer segmental dynamics.[25,30,72] Such findings provide insights for tuning the anion−cation and anion−Li interactions to achieve simultaneously high conductivities and lithium transference numbers.

■ ASSOCIATED CONTENT

Supporting Information

The Supporting Information is available free of charge at https://pubs.acs.org/doi/10.1021/acs.macromol.0c01444.

(Section S1) The Nernst−Einstein (NE) conductivity for monomeric ILs and polyILs, (Section S2) the backbone (C−C−C−C) dihedral auto-correlation functions $C_{\Phi\Phi}(t)$ under different lithium concentrations c_{Li} and the corresponding Kohlrausch−Williams−Watts (KWW) fittings, (Section S3) the characterizing anion hopping events, (Section S4) the intermittent ion pair auto-correlation function $C(t)$ and the corresponding relaxation timescale τ_c for Type1 and Type2 anions, and (Section S5) the lithium coordination characteristics in monomeric IL systems (PDF)

■ AUTHOR INFORMATION

Corresponding Author

Venkat Ganesan − *McKetta Department of Chemical Engineering, University of Texas at Austin, Austin, Texas 78712, United States;* orcid.org/0000-0003-3899-5843; Email: venkat@che.utexas.edu

Authors

Zidan Zhang − *McKetta Department of Chemical Engineering, University of Texas at Austin, Austin, Texas 78712, United States;* orcid.org/0000-0002-6909-8742

Amir T. Nasrabadi − *McKetta Department of Chemical Engineering, University of Texas at Austin, Austin, Texas 78712, United States*

Dipak Aryal − *McKetta Department of Chemical Engineering, University of Texas at Austin, Austin, Texas 78712, United States*

Complete contact information is available at: https://pubs.acs.org/10.1021/acs.macromol.0c01444

Notes

The authors declare no competing financial interest.

■ ACKNOWLEDGMENTS

The authors' works on the topic of ion transport in polymer electrolytes have been generously supported by grants from the Robert A. Welch Foundation (grant F1599) and the National Science Foundation (CBET-1706968 and DMR-1721512). The authors acknowledge the Texas Advanced Computing Center (TACC) for the generous allocation of computing resources.

■ REFERENCES

(1) Ohno, H. Functional Design of Ionic Liquids. *Bull. Chem. Soc. Jpn.* **2006**, *79*, 1665−1680.

(2) Matsumi, N.; Sugai, K.; Miyake, M.; Ohno, H. Polymerized Ionic Liquids via Hydroboration Polymerization as Single Ion Conductive Polymer Electrolytes. *Macromolecules* **2006**, *39*, 6924−6927.

(3) Mecerreyes, D. Polymeric ionic liquids: Broadening the properties and applications of polyelectrolytes. *Prog. Polym. Sci.* **2011**, *36*, 1629−1648.

(4) Kim, O.; Kim, S. Y.; Lee, J.; Park, M. J. Building Less Tortuous Ion-Conduction Pathways Using Block Copolymer Electrolytes with a Well-Defined Cubic Symmetry. *Chem. Mater.* **2016**, *28*, 318−325.

(5) Ohno, H.; Ito, K. Room-Temperature Molten Salt Polymers as a Matrix for Fast Ion Conduction. *Chem. Lett.* **1998**, *27*, 751−752.

(6) Ohno, H. Molten salt type polymer electrolytes. *Electrochim. Acta* **2001**, *46*, 1407−1411.

(7) Yuan, J.; Mecerreyes, D.; Antonietti, M. Poly(ionic liquid)s: An update. *Prog. Polym. Sci.* **2013**, *38*, 1009−1036.

(8) Choi, J.-H.; Ye, Y.; Elabd, Y. A.; Winey, K. I. Network Structure and Strong Microphase Separation for High Ion Conductivity in Polymerized Ionic Liquid Block Copolymers. *Macromolecules* **2013**, *46*, 5290−5300.

(9) Shaplov, A. S.; Ponkratov, D. O.; Aubert, P.-H.; Lozinskaya, E. I.; Plesse, C.; Vidal, F.; Vygodskii, Y. S. A first truly all-solid state organic electrochromic device based on polymeric ionic liquids. *Chem. Commun.* **2014**, *50*, 3191−3193.

(10) Yu, Y.; Lu, F.; Sun, N.; Wu, A.; Pan, W.; Zheng, L. Single lithium-ion polymer electrolytes based on poly(ionic liquid)s for lithium-ion batteries. *Soft Matter* **2018**, *14*, 6313−6319.

(11) Huang, T.; Long, M.-C.; Wu, G.; Wang, Y.-Z.; Wang, X.-L. Poly(ionic liquid)-Based Hybrid Hierarchical Free-Standing Electrolytes with Enhanced Ion Transport and Fire Retardancy Towards Long-Cycle-Life and Safe Lithium Batteries. *ChemElectroChem* **2019**, *6*, 3674−3683.

(12) Nishimura, N.; Ohno, H. 15th anniversary of polymerised ionic liquids. *Polymer* **2014**, *55*, 3289−3297.

(13) Ganesan, V. Ion transport in polymeric ionic liquids: recent developments and open questions. *Mol. Syst. Des. Eng.* **2019**, *4*, 280−293.

(14) Schauser, N. S.; Seshadri, R.; Segalman, R. A. Multivalent ion conduction in solid polymer systems. *Mol. Syst. Des. Eng.* **2019**, *4*, 263−279.

(15) Wang, X.; Kerr, R.; Chen, F.; Goujon, N.; Pringle, J. M.; Mecerreyes, D.; Forsyth, M.; Howlett, P. C. Toward High-Energy-Density Lithium Metal Batteries: Opportunities and Challenges for Solid Organic Electrolytes. *Adv. Mater.* **2020**, *32*, 1905219.

(16) Zhang, H.; Liu, C.; Zheng, L.; Feng, W.; Zhou, Z.; Nie, J. Solid polymer electrolyte comprised of lithium salt/ether functionalized ammonium-based polymeric ionic liquid with bis(fluorosulfonyl)imide. *Electrochim. Acta* **2015**, *159*, 93−101.

(17) Wang, A.; Xu, H.; Liu, X.; Gao, R.; Wang, S.; Zhou, Q.; Chen, J.; Liu, X.; Zhang, L. The synthesis of a hyperbranched star polymeric ionic liquid and its application in a polymer electrolyte. *Polym. Chem.* **2017**, *8*, 3177−3185.

(18) Wang, A.; Liu, X.; Wang, S.; Chen, J.; Xu, H.; Xing, Q.; Zhang, L. Polymeric ionic liquid enhanced all-solid-state electrolyte membrane for high-performance lithium-ion batteries. *Electrochim. Acta* **2018**, *276*, 184−193.

(19) Pablos, J. L.; García, N.; Garrido, L.; Catalina, F.; Corrales, T.; Tiemblo, P. Polycationic scaffolds for Li-ion anion exchange transport in ion gel polyelectrolytes. *J. Mater. Chem. A* **2018**, *6*, 11215−11225.

(20) Pablos, J. L.; García, N.; Garrido, L.; Guzmán, J.; Catalina, F.; Corrales, T.; Tiemblo, P. Highly efficient mixed Li+ transport in ion gel polycationic electrolytes. *J. Membr. Sci.* **2018**, *545*, 133−139.

(21) Brinkkötter, M.; Lozinskaya, E. I.; Ponkratov, D. O.; Vygodskii, Y.; Schmidt, D. F.; Shaplov, A. S.; Schönhoff, M. Influence of Cationic Poly(ionic liquid) Architecture on the Ion Dynamics in Polymer Gel Electrolytes. *J. Phys. Chem. C* **2019**, *123*, 13225−13235.

(22) Matsumoto, A.; Del Giudice, F.; Rotrattanadumrong, R.; Shen, A. Q. Rheological Scaling of Ionic-Liquid-Based Polyelectrolytes in Ionic Liquid Solutions. *Macromolecules* **2019**, *52*, 2759−2771.
(23) Wang, X.; Chen, F.; Girard, G. M. A.; Zhu, H.; MacFarlane, D. R.; Mecerreyes, D.; Armand, M.; Howlett, P. C.; Forsyth, M. Poly(Ionic Liquid)s-in-Salt Electrolytes with Co-coordination-Assisted Lithium-Ion Transport for Safe Batteries. *Joule* **2019**, *3*, 2687−2702.
(24) Borodin, O.; Smith, G. D.; Henderson, W. Li^+ Cation Environment, Transport, and Mechanical Properties of the LiTFSI Doped N-Methyl-N-alkylpyrrolidinium$^+$TFSI$^-$ Ionic Liquids. *J. Phy. Chem. B* **2006**, *110*, 16879−16886.
(25) Borodin, O.; Smith, G. D.; Geiculescu, O.; Creager, S. E.; Hallac, B.; DesMarteau, D. Li+ Transport in Lithium Sulfonylimide-Oligo-(ethylene oxide) Ionic Liquids and Oligo(ethylene oxide) Doped with LiTFSI. *J. Phys. Chem. B* **2006**, *110*, 24266−24274.
(26) Maitra, A.; Heuer, A. Cation Transport in Polymer Electrolytes: A Microscopic Approach. *Phys. Rev. Lett.* **2007**, *98*, 227802.
(27) Diddens, D.; Heuer, A.; Borodin, O. Understanding the Lithium Transport within a Rouse-Based Model for a PEO/LiTFSI Polymer Electrolyte. *Macromolecules* **2010**, *43*, 2028−2036.
(28) Sethuraman, V.; Mogurampelly, S.; Ganesan, V. Ion transport mechanisms in lamellar phases of salt-doped PS−PEO block copolymer electrolytes. *Soft Matter* **2017**, *13*, 7793−7803.
(29) Sethuraman, V.; Mogurampelly, S.; Ganesan, V. Multiscale Simulations of Lamellar PS−PEO Block Copolymers Doped with $LiPF_6$ Ions. *Macromolecules* **2017**, *50*, 4542−4554.
(30) Borodin, O.; Smith, G. D. Molecular Dynamics Simulations of Poly(ethylene oxide)/LiI Melts. 1. Structural and Conformational Properties. *Macromolecules* **1998**, *31*, 8396−8406.
(31) Mogurampelly, S.; Keith, J. R.; Ganesan, V. Mechanisms Underlying Ion Transport in Polymerized Ionic Liquids. *J. Am. Chem. Soc.* **2017**, *139*, 9511−9514.
(32) Keith, J. R.; Mogurampelly, S.; Aldukhi, F.; Wheatle, B. K.; Ganesan, V. Influence of molecular weight on ion-transport properties of polymeric ionic liquids. *Phys. Chem. Chem. Phys.* **2017**, *19*, 29134−29145.
(33) Keith, J. R.; Mogurampelly, S.; Wheatle, B. K.; Ganesan, V. Influence of side chain linker length on ion-transport properties of polymeric ionic liquids. *J. Polym. Sci., Part B: Polym. Phys.* **2017**, *55*, 1718−1723.
(34) Keith, J. R.; Ganesan, V. Ion transport in backbone-embedded polymerized ionic liquids. *J. Chem. Phys.* **2019**, *151*, 124902.
(35) Liu, H.; Maginn, E. Effect of ion structure on conductivity in lithium-doped ionic liquid electrolytes: A molecular dynamics study. *J. Chem. Phys.* **2013**, *139*, 114508.
(36) Haskins, J. B.; Bennett, W. R.; Wu, J. J.; Hernández, D. M.; Borodin, O.; Monk, J. D.; Bauschlicher, C. W., Jr.; Lawson, J. W. Computational and Experimental Investigation of Li-Doped Ionic Liquid Electrolytes: [pyr14][TFSI], [pyr13][FSI], and [EMIM][BF_4]. *J. Phys. Chem. B* **2014**, *118*, 11295−11309.
(37) Lesch, V.; Jeremias, S.; Moretti, A.; Passerini, S.; Heuer, A.; Borodin, O. A Combined Theoretical and Experimental Study of the Influence of Different Anion Ratios on Lithium Ion Dynamics in Ionic Liquids. *J. Phy. Chem. B* **2014**, *118*, 7367−7375.
(38) Molinari, N.; Mailoa, J. P.; Kozinsky, B. General Trend of a Negative Li Effective Charge in Ionic Liquid Electrolytes. *J. Phys. Chem. Letters* **2019**, *10*, 2313−2319.
(39) Huang, Q.; Lourenço, T. C.; Costa, L. T.; Zhang, Y.; Maginn, E. J.; Gurkan, B. Solvation Structure and Dynamics of Li+ in Ternary Ionic Liquid−Lithium Salt Electrolytes. *J. Phys. Chem. B* **2019**, *123*, 516−527.
(40) Nürnberg, P.; Lozinskaya, E. I.; Shaplov, A. S.; Schönhoff, M. Li Coordination of a Novel Asymmetric Anion in Ionic Liquid-in-Li Salt Electrolytes. *J. Phys. Chem. B* **2020**, *124*, 861−870.
(41) Molinari, N.; Kozinsky, B. Chelation-Induced Reversal of Negative Cation Transference Number in Ionic Liquid Electrolytes. *J. Phys. Chem. B* **2020**, *124*, 2676−2684.
(42) Tong, J.; Wu, S.; von Solms, N.; Liang, X.; Huo, F.; Zhou, Q.; He, H.; Zhang, S. The Effect of Concentration of Lithium Salt on the Structural and Transport Properties of Ionic Liquid-Based Electrolytes. *Front. Chem.* **2020**, *7*, 945.
(43) Kubisiak, P.; Wróbel, P.; Eilmes, A. Molecular Dynamics Investigation of Correlations in Ion Transport in MeTFSI/EMIM−TFSI (Me = Li, Na) Electrolytes. *J. Phys. Chem. B* **2020**, *124*, 413−421.
(44) Yoon, H.; Best, A. S.; Forsyth, M.; MacFarlane, D. R.; Howlett, P. C. Physical properties of high Li-ion content N-propyl-N-methyl-pyrrolidinium bis(fluorosulfonyl)imide based ionic liquid electrolytes. *Phys. Chem. Chem. Phys.* **2015**, *17*, 4656−4663.
(45) Chen, F.; Forsyth, M. Computational Investigation of Mixed Anion Effect on Lithium Coordination and Transport in Salt Concentrated Ionic Liquid Electrolytes. *J. Phys. Chem. Lett.* **2019**, *10*, 7414−7420.
(46) Delhorbe, V.; Bresser, D.; Mendil-Jakani, H.; Rannou, P.; Bernard, L.; Gutel, T.; Lyonnard, S.; Picard, L. Unveiling the Ion Conduction Mechanism in Imidazolium-Based Poly(ionic liquids): A Comprehensive Investigation of the Structure-to-Transport Interplay. *Macromolecules* **2017**, *50*, 4309−4321.
(47) Pronk, S.; et al. GROMACS 4.5: a high-throughput and highly parallel open source molecular simulation toolkit. *Bioinformatics* **2013**, *29*, 845−854.
(48) Jorgensen, W. L.; Maxwell, D. S.; Tirado-Rives, J. Development and Testing of the OPLS All-Atom Force Field on Conformational Energetics and Properties of Organic Liquids. *J. Am. Chem. Soc.* **1996**, *118*, 11225−11236.
(49) Santangelo, G.; Di Matteo, A.; Müller-Plathe, F.; Milano, G. From Mesoscale Back to Atomistic Models: A Fast Reverse-Mapping Procedure for Vinyl Polymer Chains. *J. Phys. Chem. B* **2007**, *111*, 2765−2773.
(50) Zhang, Z.; Wang, L.; Wang, Z.; He, X.; Chen, Y.; Müller-Plathe, F.; Böhm, M. C. A coarse-grained molecular dynamics - reactive Monte Carlo approach to simulate hyperbranched polycondensation. *RSC Adv.* **2014**, *4*, 56625−56636.
(51) Krajniak, J.; Pandiyan, S.; Nies, E.; Samaey, G. Generic Adaptive Resolution Method for Reverse Mapping of Polymers from Coarse-Grained to Atomistic Descriptions. *J. Chem. Theory Comput.* **2016**, *12*, 5549−5562.
(52) Krajniak, J.; Zhang, Z.; Pandiyan, S.; Nies, E.; Samaey, G. Reverse mapping method for complex polymer systems. *J. Comput. Chem.* **2018**, *39*, 648−664.
(53) Krajniak, J.; Zhang, Z.; Pandiyan, S.; Nies, E.; Samaey, G. Coarse-grained molecular dynamics simulations of polymerization with forward and backward reactions. *J. Comput. Chem.* **2018**, *39*, 1764−1778.
(54) Zhang, Z.; Krajniak, J.; Samaey, G.; Nies, E. A Parallel Multiscale Simulation Framework for Complex Polymerization: AB_2-Type Monomer Hyperbranched Polymerization as an Example. *Adv. Theory Simul.* **2018**, *2*, 1800102.
(55) Zhang, Z.; Krajniak, J.; Keith, J. R.; Ganesan, V. Mechanisms of Ion Transport in Block Copolymeric Polymerized Ionic Liquids. *ACS Macro Lett.* **2019**, 1096−1101.
(56) Larsen, G. S.; Lin, P.; Hart, K. E.; Colina, C. M. Molecular Simulations of PIM-1-like Polymers of Intrinsic Microporosity. *Macromolecules* **2011**, *44*, 6944−6951.
(57) Hart, K. E.; Abbott, L. J.; McKeown, N. B.; Colina, C. M. Toward Effective CO_2/CH_4 Separations by Sulfur-Containing PIMs via Predictive Molecular Simulations. *Macromolecules* **2013**, *46*, 5371−5380.
(58) Essmann, U.; Perera, L.; Berkowitz, M. L.; Darden, T.; Lee, H.; Pedersen, L. G. A smooth particle mesh Ewald method. *J. Chem. Phys.* **1995**, *103*, 8577−8593.
(59) Bhargava, B. L.; Balasubramanian, S. Refined potential model for atomistic simulations of ionic liquid [bmim][PF6]. *J. Chem. Phys.* **2007**, *127*, 114510.
(60) Keith, J. R.; Rebello, N. J.; Cowen, B. J.; Ganesan, V. Influence of Counterion Structure on Conductivity of Polymerized Ionic Liquids. *ACS Macro Lett.* **2019**, *8*, 387−392.
(61) Keith, J. R.; Ganesan, V. Ion transport mechanisms in salt-doped polymerized zwitterionic electrolytes. *J. Polym. Sci.* **2020**, *58*, 578−588.

https://dx.doi.org/10.1021/acs.macromol.0c01444
Macromolecules 2020, 53, 6995−7008

(62) Bussi, G.; Donadio, D.; Parrinello, M. Canonical sampling through velocity rescaling. *J. Chem. Phys.* **2007**, *126*, No. 014101.
(63) Basconi, J. E.; Shirts, M. R. Effects of Temperature Control Algorithms on Transport Properties and Kinetics in Molecular Dynamics Simulations. *J. Chem. Theory Comput.* **2013**, *9*, 2887−2899.
(64) Parrinello, M.; Rahman, A. Polymorphic transitions in single crystals: A new molecular dynamics method. *J. Appl. Phys.* **1981**, *52*, 7182.
(65) Doherty, B.; Zhong, X.; Gathiaka, S.; Li, B.; Acevedo, O. Revisiting OPLS Force Field Parameters for Ionic Liquid Simulations. *J. Chem. Theory Comput.* **2017**, *13*, 6131−6145.
(66) Acevedo, O. *Ionic liquid force field parameters (OPLS-2009IL and OPLS-VSIL)*; 2018> (accessed Dec 24, 2019); https://github.com/orlandoacevedo/IL.
(67) Sambasivarao, S. V.; Acevedo, O. Development of OPLS-AA Force Field Parameters for 68 Unique Ionic Liquids. *J. Chem. Theory Comput.* **2009**, *5*, 1038−1050.
(68) Zhang, Z.; Wheatle, B. K.; Krajniak, J.; Keith, J. R.; Ganesan, V. Ion Mobilities, Transference Numbers, and Inverse Haven Ratios of Polymeric Ionic Liquids. *ACS Macro Lett.* **2020**, *9*, 84−89.
(69) Chen, F.; Howlett, P.; Forsyth, M. Na-Ion Solvation and High Transference Number in Superconcentrated Ionic Liquid Electrolytes: A Theoretical Approach. *J. Phys. Chem. C* **2018**, *122*, 105−114.
(70) Borodin, O.; Smith, G. D.; Bandyopadhyaya, R.; Byutner, O. Molecular Dynamics Study of the Influence of Solid Interfaces on Poly(ethylene oxide) Structure and Dynamics. *Macromolecules* **2003**, *36*, 7873−7883.
(71) Ndoro, T. V. M.; Böhm, M. C.; Müller-Plathe, F. Interface and Interphase Dynamics of Polystyrene Chains near Grafted and Ungrafted Silica Nanoparticles. *Macromolecules* **2012**, *45*, 171−179.
(72) Mogurampelly, S.; Ganesan, V. Effect of Nanoparticles on Ion Transport in Polymer Electrolytes. *Macromolecules* **2015**, *48*, 2773−2786.
(73) Mogurampelly, S.; Sethuraman, V.; Pryamitsyn, V.; Ganesan, V. Influence of nanoparticle-ion and nanoparticle-polymer interactions on ion transport and viscoelastic properties of polymer electrolytes. *J. Chem. Phys.* **2016**, *144*, 154905.
(74) Williams, G.; Watts, D. C. Non-symmetrical dielectric relaxation behaviour arising from a simple empirical decay function. *Trans. Faraday Soc.* **1970**, *66*, 80−85.
(75) Harmandaris, V. A.; Floudas, G.; Kremer, K. Temperature and Pressure Dependence of Polystyrene Dynamics through Molecular Dynamics Simulations and Experiments. *Macromolecules* **2011**, *44*, 393−402.
(76) Lukichev, A. Physical meaning of the stretched exponential Kohlrausch function. *Phys. Lett. A* **2019**, *383*, 2983−2987.
(77) Pitawala, J.; Martinelli, A.; Johansson, P.; Jacobsson, P.; Matic, A. Coordination and interactions in a Li-salt doped ionic liquid. *J. Non-Cryst. Solids* **2015**, *407*, 318−323.
(78) Nasrabadi, A. T.; Ganesan, V. Structure and Transport Properties of Lithium-Doped Aprotic and Protic Ionic Liquid Electrolytes: Insights from Molecular Dynamics Simulations. *J. Phys. Chem. B* **2019**, *123*, 5588−5600.
(79) Mogurampelly, S.; Ganesan, V. Ion Transport in Polymerized Ionic Liquid−Ionic Liquid Blends. *Macromolecules* **2018**, *51*, 9471−9483.

https://dx.doi.org/10.1021/acs.macromol.0c01444
Macromolecules 2020, 53, 6995−7008